

pubs.acs.org/NanoLett Letter

Room-Temperature Photochromism of Silicon Vacancy Centers in **CVD Diamond**

Alexander Wood, Artur Lozovoi, Zi-Huai Zhang, Sachin Sharma, Gabriel I. López-Morales, Harishankar Jayakumar, Nathalie P. de Leon, and Carlos A. Meriles*



Cite This: Nano Lett. 2023, 23, 1017-1022



20 μm

Fluorescence (kcts/s)

ACCESS I

III Metrics & More

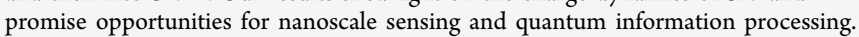
Article Recommendations

Supporting Information

532 nm

laser

ABSTRACT: The silicon vacancy (SiV) center in diamond is typically found in three stable charge states, SiV⁰, SiV⁻, and SiV²⁻, but studying the processes leading to their formation is challenging, especially at room temperature, due to their starkly different photoluminescence rates. Here, we use confocal fluorescence microscopy to activate and probe charge interconversion between all three charge states under ambient conditions. In particular, we witness the formation of SiV⁰ via the two-step capture of diffusing, photogenerated holes, a process we expose both through direct SiV⁰ fluorescence measurements at low temperatures and confocal microscopy observations in the presence of externally applied electric fields. In addition, we show that continuous red illumination induces the converse process, first transforming SiV⁰ into SiV⁻ and then into SiV2-. Our results shed light on the charge dynamics of SiV and



KEYWORDS: diamond, silicon vacancy centers, charge dynamics, color center photochromism

pin-active color centers in wide-bandgap semiconductors have emerged as a valuable platform for applications in quantum communication, computing, and sensing thanks to their long coherence lifetimes and optical access. Among the best-known examples are the nitrogen vacancy (NV) center in diamond and the divacancy center in silicon carbide, whose optical and spin properties have been the subject of extensive studies.¹⁻⁵ Part of this effort has also been devoted at identifying alternative color centers that can potentially outperform more established systems.⁶ One illustration is the silicon vacancy (SiV) center in diamond, singled out in recent years as a promising spin qubit candidate with superior optical properties.^{7–9} In particular, the neutral (SiV⁰) and negatively charged (SiV⁻) states exhibit photochromism (with emission at 946 and 737 nm) and possess optically accessible electron spins (S = 1 and 1/2), a high Debye-Waller factor, and an inversion symmetry that protects optical transitions from electric noise. 10 This allows their use close to the host crystal surface and reduces spectral diffusion of the zero-phonon line (ZPL), critical in quantum information processing and sensing applications. The SiV center can also be found in the doubly negative state (SiV²⁻), which is nonfluorescent and spinless.11,12

Among these alternative charge states, SiV⁰ is of especial interest as it exhibits much longer spin coherence times than SiV due to the absence of strong phonon-mediated spin relaxation processes. 13,14 First identified as the KUL1 center in chemical vapor deposition (CVD) diamond via electron

paramagnetic resonance, 15,16 SiV⁰ was subsequently associated with a 946 nm (1.31 eV) zero-phonon line in the photoluminescence spectrum, 17,18 only detectable below ~240 K in ensembles due to the suppression of otherwise dominant nonradiative processes. Long spin coherence and spin-lattice relaxation times—comparable to those found in NVs¹—have recently been observed below 20 K using pulsed electron paramagnetic resonance 14,19 and optically detected magnetic

Despite much progress, stabilizing the SiV charge state into SiV⁰ remains a challenging problem. First-principles calculations indicate that the preferred SiV charge states in synthetic diamond are SiV or SiV2-.11,12 It has been shown that boron doping during crystal growth shifts the Fermi level to favor the formation of SiV⁰. 14 Alternatively, hydrogen termination of the diamond surface has been exploited to induce the local formation of shallow SiV⁰ centers with properties similar to those found in the bulk of the crystal.²

Here we pay particular attention to processes of charge state conversion based on recombination of itinerant free carriers, which can be created via photoionization of nearby defects.

Received: November 16, 2022 Revised: January 13, 2023 Published: January 20, 2023





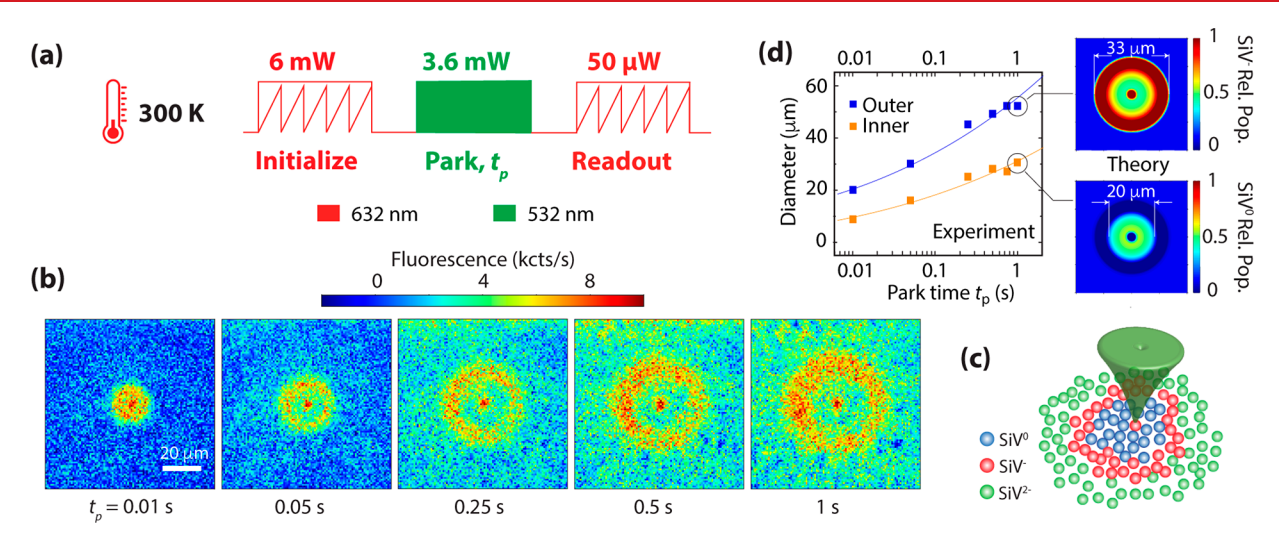


Figure 1. Photoinduced formation of SiV^0 under ambient conditions. (a) SiV^- preparation and detection protocol at room temperature; upon a red laser scan (632 nm at 6 mW, $80 \times 80 \mu m^2$) and a green park (532 nm at 3.6 mW) for a variable time t_p , we image the resulting SiV^- distribution via a weak red laser scan (632 nm at $50 \mu W$, 10 ms per pixel, 100×100 pixels). (b) SiV^- images as derived from the protocol in (a). (c) Schematics of charge dynamics under a green laser park; the inner blue ring signals the formation of SiV^0 via double hole capture. (d) (left) Time dependence of the outer and inner radii in the measured charge patterns; solid lines are guides to the eye. (right) Calculated SiV^- and SiV^0 relative populations (top and bottom plots, respectively) for the conditions in (b) assuming a park time of 1 s.

This form of "photodoping"—successfully demonstrated with NV centers^{22,23}—has been shown to produce long-lived, nonequilibrium charge state distributions when the concentration of nitrogen impurities is moderate (~1 ppm or less).²⁴ Subsequent experiments on SiVs showed that 532 or 632 nm illumination generates free carriers that are then captured outside the illumination region, resulting in the generation of a characteristic SiV "bright halo". 25,26 Identification of the charge carrier responsible for the observed effect is hindered by the fact that both SiV⁰ and SiV²⁻ are dark at room temperature. Experiments in the presence of external electric fields suggested that electron capture by SiV⁰ plays a key role in the formation of the halo.²⁶ It was later argued, however, that annealed CVD diamond favors the formation of SiV²⁻, not SiV⁰, as the predominant charge state.²⁷ The notion of SiV²⁻ as the charge state "by default" gained support in recent experiments exploiting individual NV centers as charge sensors to reveal the sign of carriers photoactivated from proximal SiVs.²⁸

In this work, we identify the conditions for the formation of all three SiV charge states—SiV⁰, SiV⁻, and SiV²⁻—under ambient conditions. We use multicolor confocal microscopy to image the SiV⁻ charge state distribution at room temperature after exposure to photogenerated charge carriers and confirm the inferred charge states by direct detection of SiV⁰ photoluminescence at 10 K. In addition, we employ electric fields to probe the effect of drifting carriers, which allows us to discriminate between their signs and corresponding capture processes. Finally, we examine the response under continuous red illumination and show the sequential, laser-induced transformation of SiVs from neutral, to single charged, to double-negatively charged. These room-temperature results are consistent with and complement observations under cryogenic conditions discussed in a recent study.²⁹

In our experiments, we use a CVD-grown [100] diamond with a nitrogen concentration of ~1 ppm as reported by the manufacturer (DDK). Silicon incorporates during crystal growth as a contaminant due to etching of the reactor quartz windows;³⁰ from prior studies,²⁶ we estimate the SiV and NV

concentrations at \sim 0.3 and \sim 0.03 ppm, respectively. For room-temperature measurements, we resort to a home-built confocal microscope accommodating 532 and 632 nm excitation laser paths; we use a bandpass filter to limit photon collection to a narrow window around the SiV $^-$ ZPL at 737 nm (see the Supporting Information, Section I).

The schematic in Figure 1a lays out our experimental protocol: We first implement multiple 632 nm, 6 mW laser scan across a $(80 \ \mu\text{m})^2$ area to initialize SiVs into a nonfluorescing charge state (Supporting Information, Section II). We subsequently park a 532 nm, 3.6 mW laser at the center of the scanned plane for a variable time t_p ; illumination at this wavelength is known to generate a continuous stream of free electrons and holes stemming from charge cycling of coexisting NVs. ^{31–33} The ensuing carrier diffusion and capture produces a nonlocal change of the SiV charge state, which we subsequently image under 632 nm, 50 μ W excitation.

Figure 1b shows the results for variable park times: Consistent with prior observations, 26 we first see a bright SiV halo centered around the point of illumination after only 10 ms of green excitation. Upon increasing t_p , however, we witness the formation of a dark inner ring growing concomitantly with the outer bright pattern. This alternating, concentric structure suggests a double carrier capture process where SiVs not directly exposed to the green laser become negative (and hence bright) after a first capture event, to subsequently turn dark again upon capture of a second carrier. Provided the initial red scan preferentially produces SiV²⁻, this process amounts to a double hole capture, and correspondingly implies the formation of an SiV⁰-rich ring in the region adjacent to the parked beam (see schematics in Figure 1c). Interestingly, preceding experiments missed these dynamics, instead reporting the formation of a uniformly bright SiVdisk.²⁶ We later show this is a consequence of the system's high sensitivity to the probe laser intensity, rapidly converting SiV⁰ into SiV- even at these lower powers (see also Supporting Information, Section III).

Conceptually, the formation of the observed SiV charge pattern must emerge from an interplay between carrier

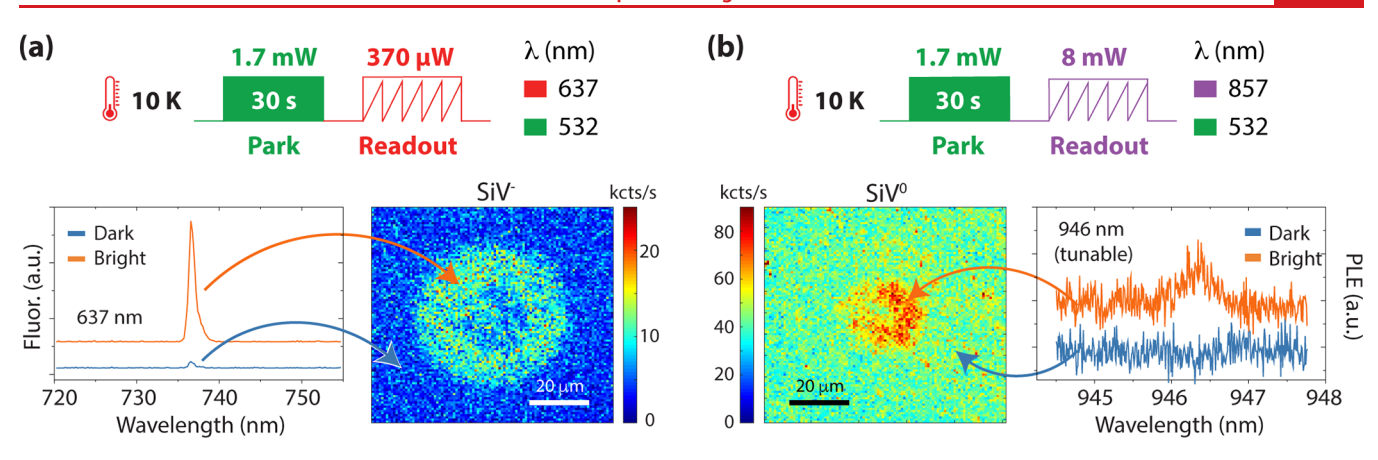


Figure 2. Direct observation of SiV⁰ formation via hole capture. (a) (top) SiV⁻ imaging protocol at cryogenic temperatures. Following a 532 nm, 1.7 mW beam park at the center for 30 s, we image the resulting SiV⁻ distribution using a 637 nm, 400 μ W beam. (bottom) Confocal imaging of SiV⁻; the orange (blue) traces in the side photoluminescence spectra show that the bright (dark) areas of the image are SiV⁻-rich (SiV⁻-depleted). (b) Same as in (a) but for SiV⁰. In this case, however, we use an 857 nm laser for image readout and obtain a photoluminescence (PLE) spectrum via a 0.3 mW laser tunable around 946 nm. The bright ring at the image center directly demonstrates formation of SiV⁰. In (a) and (b), spectra have been displaced vertically for clarity; all experiments at 10 K.

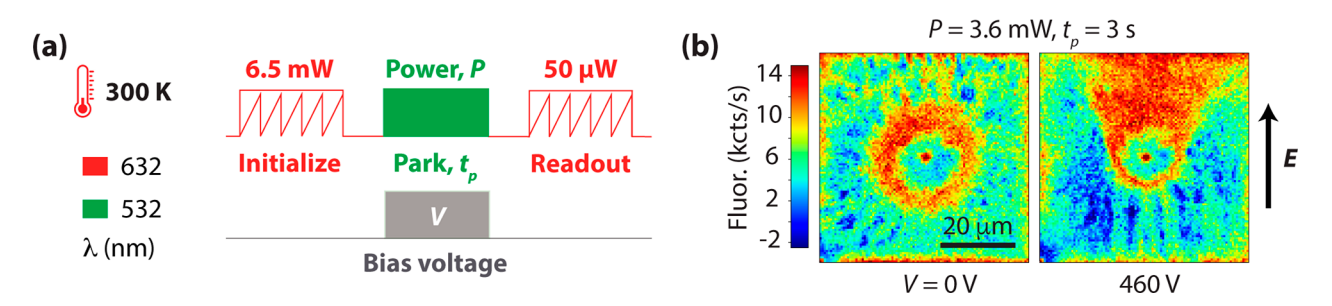


Figure 3. SiV charge state dynamics in the presence of a bias electric field. (a) Experimental protocol; we use silver planar electrodes separated by a 100 μ m gap (not shown) to produce a time-independent electric field across the imaged area during a 532 nm laser park of variable power P and duration t_p . (b) Confocal images of SiV⁻ with and without a bias voltage V for long park times (right and left images, respectively); the comet-tail-shaped pattern emerging in the presence of an external bias can be understood as the result of holes drifting under the external electric field E. Throughout these experiments, the green laser power and park duration respectively are P = 3.6 mW and $t_p = 3$ s.

photoactivation, diffusion, and capture in the presence of localized optical excitation. This interplay can, in turn, be cast in terms of a set of master equations that simultaneously take into account the presence of SiV, NV, and substitutional nitrogen (N_s) in their different charge states (Supporting Information, Section III). Indeed, N_s impurities—significantly more abundant than SiVs and NVs in CVD diamond³⁴ charge cycle between neutral and positively charged upon exposure to a stream of electrons and holes, hence playing an important role in the SiV pattern formation.^{35,36} We capture these dynamics in Figure 1d, where we compare our observations—distilled in the main plot as the experimentally measured time evolution of the outer and inner ring diameters—with numerical simulations for a 1 s park time, shown in the right inset. Consistent with our model, we find the formation of an SiV⁰-rich inner ring separated from the SiV²⁻ background by an SiV⁻ bright halo. A close inspection of the observed and calculated diameters, however, shows that the agreement is far from complete and must, therefore, be seen as qualitative. This is largely a consequence of the uncertainty surrounding the charge-state-dependent electron and hole capture cross sections for NVs, SiVs, and Ns, which in several cases are not known (Supporting Information, Section IV).

To disambiguate the composition of the inner ring, we carry out low-temperature experiments where the SiV^0 fluorescence can be monitored directly. ¹⁴ To this end, we make use of a

second cryo-workstation-based confocal microscope simultaneously integrating 532, 637, and 857 nm lasers (Supporting Information, Section I). With a wavelength above the SiV⁰ recombination threshold at ~825 nm,^{20,37} 857 nm light facilitates nondestructive detection of SiV⁰ fluorescence (too weak at room temperature due to nonradiative decay). Figures 2a and 2b respectively display SiV⁻- and SiV⁰-selective images emerging upon a prolonged (60 s) green laser park time: We find complementary fluorescence maps that confirm the distinct charge state predominant in each section of the pattern. In addition, optical spectroscopy on dark and bright sectors of either image directly indicates the formation of SiV⁰ as revealed by the emission peak near 946 nm (upper trace in the side plot of Figure 2b).

While the experiments mentioned above rely on itinerant carriers spreading from the point of photoactivation, the application of external electric fields allows us, in principle, to imprint a distinct spatial bias in the diffusion of electrons and holes, observable at room temperature. We lay out this class of experiments in Figure 3a, where we introduce a constant voltage difference across the imaged plane throughout the duration of the laser park. Figure 3b compares our observations with and without external fields: We find that the SiV⁻ ring previously observed under similar conditions (Figure 1b) reshapes into a long tail pointing toward the negative electrode. In addition, although the inner dark ring

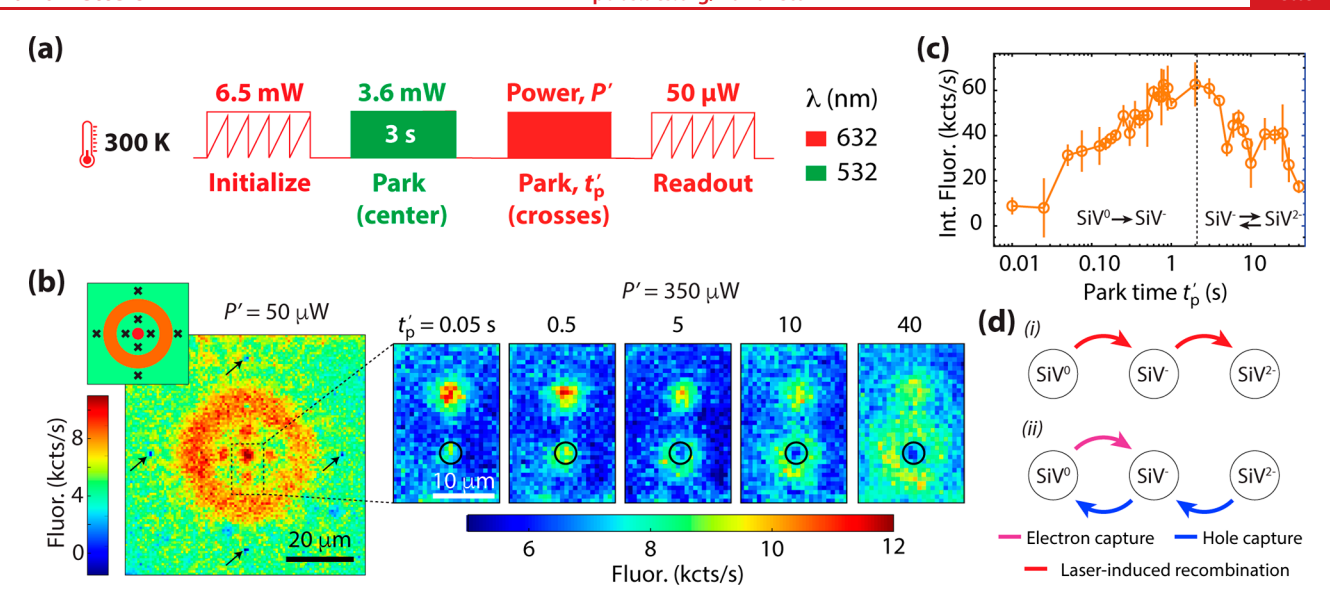


Figure 4. Charge dynamics of SiV under red illumination. (a) Experimental protocol. Following a 3 s green beam park on a red-laser-initialized background, we use a 632 nm laser to illuminate select points in the pattern. (b) Confocal image of SiV $^-$ (100 × 100 pixels, 10 ms per pixel) upon application of the protocol in (a). Crosses in the upper left insert indicate the locations of 632 nm, 50 μ W parks relative to the bright ring in the pattern for a time $t'_p = 0.5$ s. Arrows indicate the positions of the outer parks, less visible than those in the inner dark ring. The image series on the right-hand side shows zoomed-in confocal maps of the area within the dashed square. We monitor the integrated SiV $^-$ fluorescence within the black circle for variable red laser park durations ($P' = 350 \mu$ W). (c) Integrated SiV $^-$ fluorescence versus t'_p at the inner (dark) ring position highlighted in (b); red excitation first creates and then partially depletes SiV $^-$. (d) Putative SiV charge dynamics under 632 nm illumination. (i) Upon direct exposure to red light, SiV 0 first recombines into SiV $^-$ and then into SiV 2 $^-$. (ii) In the dark, SiV $^-$ formation arises from hole capture by SiV 2 $^-$ or from electron capture by SiV 0 ; one scenario or the other becomes dominant depending on the charge state initialization history.

undergoes a less dramatic transformation, a close examination also indicates bias toward the upper section of the plane, all of which is consistent with the notion of hole trapping as the driving mechanism underlying SiV⁻ formation. For completeness, we note that the observed changes in the outer sections of the fluorescence pattern—turned dark by the red initialization scan—are simply the (undesired) effect of scattered light on the red-initialized SiV ensemble and can, therefore, be ignored (Supporting Information, Section V).

At face value, the results in Figure 3 contradict some of the conclusions from our prior work²⁶ where similar experiments suggested SiV⁻ generation from electron capture by SiV⁰. Although dissimilar experimental conditions—including a different charge-state preparation history, a stronger readout beam, and the use of a vertical, not horizontal, electrode set make an in-depth comparison difficult, we suspect that one regime or the other may be dominant depending on the chosen parameter set. In particular, preliminary observations not presented here for brevity—show that local optical excitation and externally applied electric fields can combine to produce a rich, though complex, phenomenology; this includes, e.g., the formation of bidirectional, jet-like patterns where SiV⁻ formation seemingly emerges both from hole capture by SiV²⁻ in one-half of the plane and from electron capture by SiV⁰ in the other. We defer the in-depth discussion of these and related results-including an examination of the role of space charge fields in the SiV⁻ pattern formation³⁸—to an upcoming study.

Our ability to prepare SiV^0 -rich ensembles at room temperature gives us the opportunity to probe their charge dynamics in the presence of continuous optical excitation. To this end, we implement the experimental protocol in Figure 4a: Upon creating an SiV^0 -rich area, we park a 632 nm, 50 μ W laser at select, off-centered positions for a variable time, t'_p , to

subsequently reconstruct an image via a weak red scan. Figure 4b shows the result for a case where we sequentially illuminate eight different locations evenly distributed in the SiV^0 and SiV^{2-} portions of the imaged plane (crosses in the upper left diagram). We find remarkably different responses: While red illumination in the outer sections of the pattern leads to sharp, dark spots, the opposite takes place near the center where we observe bright spots emerge. The latter signals a red-induced recombination of SiV^0 into SiV^- , whereas the former points to the recombination of SiV^0 (residually present in the SiV^{2-} background after a green park; see Supporting Information, Section VI).

When combined, the observations mentioned above indicate a cascade process where red excitation first transforms SiV^0 into SiV^- and then into SiV^{2-} . We experimentally capture this full sequence by monitoring the fluorescence from a nearcenter section of the pattern upon a variable red park time (Figure 4c and side image series in Figure 4b). Following an early growth of SiV^- fluorescence $(0-1\ s)$, we subsequently find a gradual decay that we interpret as a recombination into SiV^{2-} . This light-induced charge-state progression mirrors the two-step, diffusion-driven hole capture process highlighted before and hence can be effectively seen as its converse.

Remarkably, prolonged red excitation on the SiV^0 -rich region also results in the formation of a surrounding bright halo slowly growing over time to reach an outer diameter of ~15 μ m after a 40 s park (image series in Figure 4b). Given the starting charge state composition of the ensemble, we must attribute SiV^- formation to electron capture at SiV^0 sites, presumably facilitated here by a stream of itinerant electrons produced by local $\mathrm{N_s^0}$ (and NV^-) ionization under the 632 nm laser beam. Note that SiV^0 formation during the (preceding) green park is likely accompanied by the preferential transformation of $\mathrm{N_s^0}$ (arguably abundant after the red initialization

Nano Letters pubs.acs.org/NanoLett Letter

scan) into neutral. In the absence of competing trapping sites, one would correspondingly expect the probability of electron capture by SiV^0 to grow, consistent with our observations (Figure 4d). This physical picture, of course, hinges on the assumption of a sufficiently large electron reservoir at the point of red excitation; additional, more quantitative work will therefore be needed to gain an accurate description of the charge dynamics at play.

In summary, our experiments in CVD diamond show that optical illumination combined with carrier diffusion and capture lead to the formation of fluorescence patterns segmented into areas where SiVs take different predominant charge states. In particular, we demonstrate the room-temperature formation of SiV⁰-rich disks surrounding the point of local green illumination, which we associate to a sequential hole capture process, first transforming SiV²⁻ into single-negatively charged and then into neutral. Starting with an SiV⁰ ensemble, we show that the exact converse process can take place locally under continuous 632 nm illumination. In addition, these same observations also suggest the alternative formation of SiV⁻ from itinerant electron, not hole, capture, which manifests or not depending on the charge initialization history.

Our results open up opportunities for the overall characterization of SiV charge state dynamics (including, e.g., the identification of ionization/recombination thresholds) through the combined use of microscopy and optical spectroscopy techniques. On the other hand, the ability to reversibly control the SiV charge state from neutral to double-negative and back could be exploited to engineer quantum memories through ²⁹Si-hosting color centers that can store the electronic spin state of SiV⁰ in the spinless environment created by SiV^{2-.39} In addition, the efficient hole-capture-assisted formation of SiV⁰ we observe raises the question as to whether other hitherto hidden features can be exposed at room temperature. Of particular interest are processes such as optical spin polarization and/or spin-selective recombination, which could perhaps be leveraged to optically detect SiV⁰ magnetic resonance under ambient conditions via spin-to-charge conversion protocols.

ASSOCIATED CONTENT

Supporting Information

The Supporting Information is available free of charge at https://pubs.acs.org/doi/10.1021/acs.nanolett.2c04514.

Additional information about sample characteristics and instrumentation used; additional details on the Monte Carlo modeling (PDF)

AUTHOR INFORMATION

Corresponding Author

Carlos A. Meriles — Department. of Physics, CUNY-City College of New York, New York, New York 10031, United States; CUNY-Graduate Center, New York, New York 10016, United States; orcid.org/0000-0003-2197-1474; Email: cmeriles@ccny.cuny.edu

Authors

Alexander Wood — Department. of Physics, CUNY-City College of New York, New York, New York 10031, United States; University of Melbourne, Parkville, VIC 3010, Australia Artur Lozovoi — Department. of Physics, CUNY-City College of New York, New York, New York 10031, United States;
orcid.org/0000-0002-6003-3168

Zi-Huai Zhang — Department of Electrical and Computer Engineering, Princeton University, Princeton, New Jersey 08544, United States; oorcid.org/0000-0001-7999-9790

Sachin Sharma – Department. of Physics, CUNY-City College of New York, New York, New York 10031, United States

Gabriel I. López-Morales — Department. of Physics, CUNY-City College of New York, New York, New York 10031, United States

Harishankar Jayakumar — Department. of Physics, CUNY-City College of New York, New York, New York 10031, United States; University of Minnesota, Minneapolis, Minnesota 55455, United States

Nathalie P. de Leon — Department of Electrical and Computer Engineering, Princeton University, Princeton, New Jersey 08544, United States; orcid.org/0000-0003-1324-1412

Complete contact information is available at: https://pubs.acs.org/10.1021/acs.nanolett.2c04514

Author Contributions

A.W. and A.L. contributed equally to this work.

Notes

The authors declare no competing financial interest.

ACKNOWLEDGMENTS

All authors acknowledge support by the U.S. Department of Energy, Office of Science, National Quantum Information Science Research Centers, Co-design Center for Quantum Advantage (C2QA) under Contract DE-SC0012704. A.W., A.L., S.S., H.J., and C.A.M. acknowledge access to the facilities and research infrastructure of NSF CREST-IDEALS, Grant NSF-HRD-1547830. A.W. was additionally supported by the Australian Research Council (Grant ID DE210101093).

■ REFERENCES

- (1) Doherty, M. W.; Manson, N. B.; Delaney, P.; Jelezko, F.; Wrachtrup, J.; Hollenberg, L. C. The nitrogen-vacancy colour centre in diamond. *Phys. Rep.* **2013**, *528*, 1–45.
- (2) Pompili, M.; Hermans, S. L. N.; Baier, S.; Beukers, H. K. C.; Humphreys, P. C.; Schouten, R. N.; Vermeulen, R. F. L.; Tiggelman, M. J.; dos Santos Martins, L.; Dirkse, B.; Wehner, S.; Hanson, R.w Realization of a multinode quantum network of remote solid-state qubits. *Science* **2021**, *372*, 259–264.
- (3) Bradley, C. E.; Randall, J.; Abobeih, M. H.; Berrevoets, R. C.; Degen, M. J.; Bakker, M. A.; Markham, M.; Twitchen, D. J.; Taminiau, T. H. A ten-qubit solid-state spin register with quantum memory up to one minute. *Phys. Rev. X* **2019**, *9*, 031045.
- (4) Christle, D. J.; Klimov, P. V.; Charles, F.; Szász, K.; Ivády, V.; Jokubavicius, V.; Hassan, J. U.; Syväjärvi, M.; Koehl, W. F.; Ohshima, T.; Son, N. T.; Janzen, E.; Gali, A.; Awschalom, D. D. Isolated spin qubits in SiC with a high-fidelity infrared spin-to-photon interface. *Phys. Rev. X* **2017**, *7*, 021046.
- (5) Anderson, C. P.; Glen, E. O.; Zeledon, C.; Bourassa, A.; Jin, Y.; Zhu, Y.; Vorwerk, C.; Crook, A. L.; Abe, H.; Ul-Hassan, J.; Ohshima, T.; Son, N. T.; Galli, G.; Awschalom, D. D. Five-second coherence of a single spin with single-shot readout in silicon carbide. *Sci. Adv.* **2022**, 8. eabm 5912.
- (6) Wolfowicz, G.; Heremans, F. J.; Anderson, C. P.; Kanai, S.; Seo, H.; Gali, A.; Galli, G.; Awschalom, D. D. Quantum guidelines for solid-state spin defects. *Nat. Rev. Mater.* **2021**, *6*, 906.

- (7) Hepp, C.; Müller, T.; Waselowski, V.; Becker, J. N.; Pingault, B.; Sternschulte, H.; Steinmüller-Nethl, D.; Gali, A.; Maze, J. R.; Atatüre, M.; Becher, C. Electronic structure of the silicon vacancy color center in diamond. *Phys. Rev. Lett.* **2014**, *112*, 036405.
- (8) Sipahigil, A.; Jahnke, K. D.; Rogers, L. J.; Teraji, T.; Isoya, J.; Zibrov, A. S.; Jelezko, F.; Lukin, M. D. Indistinguishable photons from separated silicon-vacancy centers in diamond. *Phys. Rev. Lett.* **2014**, *113*, 113602.
- (9) Sukachev, D. D.; Sipahigil, A.; Nguyen, C. T.; Bhaskar, M. K.; Evans, R. E.; Jelezko, F.; Lukin, M. D. Silicon-vacancy spin qubit in diamond: a quantum memory exceeding 10 ms with single-shot state readout. *Phys. Rev. Lett.* **2017**, *119*, 223602.
- (10) Dietrich, A.; Jahnke, K. D.; Binder, J. M.; Teraji, T.; Isoya, J.; Rogers, L. J.; Jelezko, F. Isotopically varying spectral features of silicon-vacancy in diamond. *New J. Phys.* **2014**, *16*, 113019.
- (11) Gali, A.; Maze, J. R. Ab initio study of the split silicon-vacancy defect in diamond: Electronic structure and related properties. *Phys. Rev. B* **2013**, *88*, 235205.
- (12) Thiering, G.; Gali, A. Ab Initio Magneto-Optical Spectrum of Group-IV Vacancy Color Centers in Diamond. *Phys. Rev. X* **2018**, *8*, 021063.
- (13) Jahnke, K. D.; Sipahigil, A.; Binder, J. M.; Doherty, M. W.; Metsch, M.; Rogers, L. J.; Manson, N. B.; Lukin, M. D.; Jelezko, F. Electron—phonon processes of the silicon-vacancy centre in diamond. *New J. Phys.* **2015**, *17*, 043011.
- (14) Rose, B. C.; Huang, D.; Zhang, Z. H.; Stevenson, P.; Tyryshkin, A. M.; Sangtawesin, S.; Srinivasan, S.; Loudin, L.; Markham, M. L.; Edmonds, A. M.; Twitchen, D. J.; Lyon, S. A.; De Leon, N. P. Observation of an environmentally insensitive solid-state spin defect in diamond. *Science* **2018**, *361*, 60.
- (15) Iakoubovskii, K.; Stesmans, A.; Nouwen, B.; Adriaenssens, G. J. ESR and optical evidence for a Ni vacancy center in CVD diamond. *Phys. Rev. B* **2000**, *62*, 16587.
- (16) Edmonds, A. M.; Newton, M. E.; Martineau, P. M.; Twitchen, D. J.; Williams, S. D. Electron paramagnetic resonance studies of silicon-related defects in diamond. *Phys. Rev. B* **2008**, *77*, 245205.
- (17) D'Haenens-Johansson, U. F. S.; Edmonds, A. M.; Newton, M. E.; Goss, J. P.; Briddon, P. R.; Baker, J. M.; Martineau, P. M.; Khan, R. U. A.; Twitchen, D. J.; Williams, S. D. EPR of a defect in CVD diamond involving both silicon and hydrogen that shows preferential alignment. *Phys. Rev. B* **2010**, *82*, 155205.
- (18) D'Haenens-Johansson, U. F. S.; Edmonds, A. M.; Green, B. L.; Newton, M. E.; Davies, G.; Martineau, P. M.; Khan, R. U. A.; Twitchen, D. J. Optical properties of the neutral silicon split-vacancy center in diamond. *Phys. Rev. B* **2011**, *84*, 245208.
- (19) Green, B. L.; Mottishaw, S.; Breeze, B. G.; Edmonds, A. M.; D'Haenens-Johansson, U. F. S.; Doherty, M. W.; Williams, S. D.; Twitchen, D. J.; Newton, M. E. Neutral silicon-vacancy center in diamond: Spin polarization and lifetimes. *Phys. Rev. Lett.* **2017**, *119*, 096402.
- (20) Zhang, Z. H.; Stevenson, P.; Thiering, G.; Rose, B. C.; Huang, D.; Edmonds, A. M.; Markham, M. L.; Lyon, S. A.; Gali, A.; De Leon, N. P. Optically detected magnetic resonance in neutral silicon vacancy centers in diamond via bound exciton states. *Phys. Rev. Lett.* **2020**, 125, 237402.
- (21) Zhang, Z. H.; Zuber, J. A.; Rodgers, L. V.; Gui, X.; Stevenson, P.; Li, M.; Batzer, M.; Grimau, M.; Shields, B.; Edmonds, A. M.; Palmer, N.; Markham, M. L.; Cava, R. J.; Maletinsky, P.; De Leon, N. P. Neutral silicon vacancy centers in undoped diamond via surface control, 2022, 2206.13698, arXiv (accessed 2023-01-11).
- (22) Jayakumar, H.; Henshaw, J.; Dhomkar, S.; Pagliero, D.; Laraoui, A.; Manson, N. B.; Albu, R.; Doherty, M. W.; Meriles, C. A. Optical patterning of trapped charge in nitrogen-doped diamond. *Nat. Commun.* **2016**, *7*, 1–8.
- (23) Dhomkar, S.; Henshaw, J.; Jayakumar, H.; Meriles, C. A. Longterm data storage in diamond. *Sci. Adv.* **2016**, *2*, e1600911.
- (24) Collins, A. T. The Fermi level in diamond. J. Phys. Cond. Matter 2002, 14, 3743.

- (25) Jayakumar, H.; Lozovoi, A.; Daw, D.; Meriles, C. A. Long-term spin state storage using ancilla charge memories. *Phys. Rev. Lett.* **2020**, 125, 236601.
- (26) Dhomkar, S.; Zangara, P. R.; Henshaw, J.; Meriles, C. A. Ondemand generation of neutral and negatively charged silicon-vacancy centers in diamond. *Phys. Rev. Lett.* **2018**, *120*, 117401.
- (27) Breeze, B. G.; Meara, C. J.; Wu, X. X.; Michaels, C. P.; Gupta, R.; Diggle, P. L.; Dale, M. W.; Cann, B. L.; Ardon, T.; D'Haenens-Johansson, U. F. S.; Friel, I.; Rayson, M. J.; Briddon, P. R.; Goss, J. P.; Newton, M. E.; Green, B. L. Doubly charged silicon vacancy center, Si-N complexes, and photochromism in N and Si co-doped diamond. *Phys. Rev. B* **2020**, *101*, 184115.
- (28) Gardill, A.; Kemeny, I.; Cambria, M. C.; Li, Y.; Dinani, H. T.; Norambuena, A.; Maze, J. R.; Lordi, V.; Kolkowitz, S. Probing charge dynamics in diamond with an individual color center. *Nano Lett.* **2021**, *21*, 6960–6966.
- (29) Zhang, Z. H.; Edmonds, A. M.; Palmer, N.; Markham, M. L.; De Leon, N. P. Neutral silicon vacancy centers in diamond via photoactivated itinerant carriers, 2022, 2209.08710, arXiv (accessed 2023-01-11).
- (30) Tallaire, A.; Achard, J.; Secroun, A.; De Gryse, O.; De Weerdt, F.; Barjon, J.; Silva, F.; Gicquel, A. Multiple growth and characterization of thick diamond single crystals using chemical vapour deposition working in pulsed mode. *J. Cryst. Growth* **2006**, *291*, 533–539.
- (31) Aslam, N.; Waldherr, G.; Neumann, P.; Jelezko, F.; Wrachtrup, J. Photo-induced ionization dynamics of the nitrogen vacancy defect in diamond investigated by single-shot charge state detection. *New J. Phys.* **2013**, *15*, 013064.
- (32) Lozovoi, A.; Jayakumar, H.; Daw, D.; Vizkelethy, G.; Bielejec, E.; Doherty, M. W.; Flick, J.; Meriles, C. A. Optical activation and detection of charge transport between individual colour centres in diamond. *Nat. Electron.* **2021**, *4*, 717–724.
- (33) Lozovoi, A.; Vizkelethy, G.; Bielejec, E.; Meriles, C. A. Imaging dark charge emitters in diamond via carrier-to-photon conversion. *Sci. Adv.* **2022**, *8*, eabl9402.
- (34) Edmonds, A. M.; D'Haenens-Johansson, U. F. S.; Cruddace, R. J.; Newton, M. E.; Fu, K.-M. C.; Santori, C.; Beausoleil, R. G.; Twitchen, D. J.; Markham, M. L. Production of oriented nitrogenvacancy color centers in synthetic diamond. *Phys. Rev. B* **2012**, *86*, 035201
- (35) Khan, R. U. A.; Martineau, P. M.; Cann, B. L.; Newton, M. E.; Twitchen, D. J. Charge transfer effects, thermo and photochromism in single crystal CVD synthetic diamond. *J. Phys. Cond. Matter* **2009**, *21*, 364214.
- (36) Lozovoi, A.; Daw, D.; Jayakumar, H.; Meriles, C. A. Dark defect charge dynamics in bulk chemical-vapor-deposition-grown diamonds probed via nitrogen vacancy centers. *Phys. Rev. Mater.* **2020**, *4*, 053602.
- (37) Allers, L.; Collins, A. T. Photoconductive spectroscopy of diamond grown by chemical vapor deposition. *J. Appl. Phys.* **1995**, 77, 3879–3884.
- (38) Lozovoi, A.; Jayakumar, H.; Daw, D.; Lakra, A.; Meriles, C. A. Probing metastable space-charge potentials in a wide band gap semiconductor. *Phys. Rev. Lett.* **2020**, 125 (2020), 256602.
- (39) Pfender, M.; Aslam, N.; Simon, P.; Antonov, D.; Thiering, G.; Burk, S.; Fávaro de Oliveira, F.; Denisenko, A.; Fedder, H.; Meijer, J.; Garrido, J. A.; Gali, A.; Teraji, T.; Isoya, J.; Doherty, M. W.; Alkauskas, A.; Gallo, A.; Grüneis, A.; Neumann, P.; Wrachtrup, J. Protecting a diamond quantum memory by charge state control. *Nano Lett.* 2017, 17, 5931–5937.